ELSEVIER

Materials Science and Engineering A317 (2001) 70–76

MATERIALS SCIENCE & ENGINEERING A

www.elsevier.com/locate/msea

Molecularly-based numerical evaluation of free volume in amorphous polymers

Santosh Putta, Sia Nemat-Nasser *

Department of Applied Mechanics and Engineering Science, Center of Excellence for Advanced Materials, University of California, San Diego, La Jolla, CA 92093-0416, USA

Abstract

A study of the microstructure of polymers is essential for the understanding of their anomalous diffusion properties. The concept of free volume may be utilized to study relaxation phenomena and diffusion processes in polymers. Since a quantitative definition of free volume is not possible, a new concept called available volume is introduced. A simple geometric definition of available volume, relevant for the diffusion of small molecules in polymers, is given, based on the molecular structure. An initial molecular structure is obtained using a modified RIS (rotational isomeric state) approach. Then, with the aid of a molecular mechanics-based minimization procedure, computationally generated molecular structures for some polymers are used to estimate the available volume, using the proposed geometric definition. Numerically evaluated available volume distributions are then compared for different types of amorphous polymers, e.g. polycarbonates and polyacrylates, stressing their relevance to the diffusion properties.

Keywords: Diffusion; Free volume; Amorphous polymers

1. Introduction

Understanding the processes of the diffusion of small molecules in polymers is of importance in practical applications, ranging from designing better polymeric membranes to developing more durable structural polymers. This area of research has received considerable attention over the past 50 years. Yet, several anomalies (compared to linear Fickian diffusion), that have been observed in amorphous polymers, are not yet well understood. The complicated, amorphous structure of the polymers plays an important role in producing these anomalies.

In general, the diffusion of small molecules in polymers is influenced by one or more of the following three main factors: (1) available space in the structure (i.e. free volume and its distribution); (2) flexibility of the polymer chains and their side groups; and (3) interaction forces between the polymer molecules and the diffusant molecule. The observed anomalies are due to one or more of these factors. Successful modeling of diffusion processes depends on one's ability to recognize the relative importance of the above factors. Thus, a detailed analysis of the microstructure would help the understanding of the involved mechanisms. As a first step towards this goal, current work is concerned with analyzing the free space available in a polymer for diffusion, based only on its chemical structure. Since an exact quantitative definition of free volume is not possible, we introduce a new quantity called available volume, which has a specific quantitative definition, and, qualitatively, represents the free volume. Some earlier work [1,2], has focused on molecular level simulations using Transition State Theory or Molecular Dynamics using the available volume calculations. The aim of the present work is to gain an understanding of the macroscopic diffusion models that take into account the relative importance of the three main factors mentioned above.

* Corresponding author. Tel.: +1-858-5344914; fax: +1-858-5342727.

E-mail address: sia@shiba.ucsd.edu (S. Nemat-Nasser).

0921-5093/01/$ - see front matter
PII: S0921-5093(01)01181-9

2. Structure generation

A realistic molecular structure of several polymers has been obtained using molecular mechanics and molecular dynamics approaches. This procedure is based on a Modified Rotational Isomeric State (RIS) theory [3,4]. Only a brief outline of the procedure will be given. The reader is directed to the above references for details.

The following assumptions are made in computationally generating the structure:

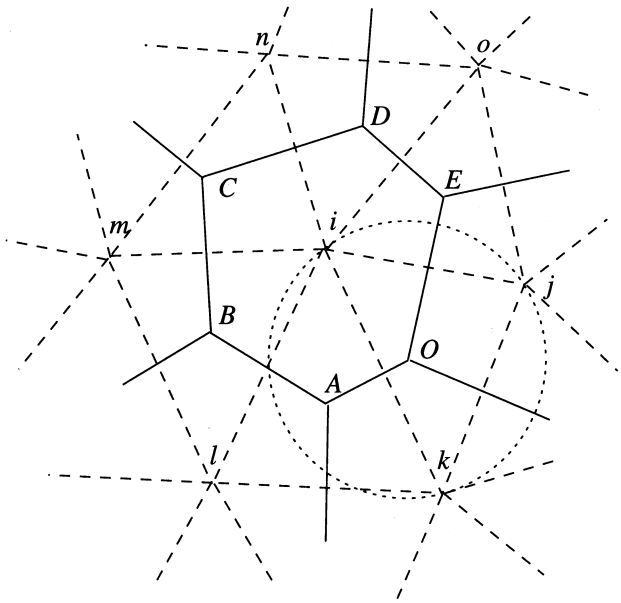

Fig. 1. Two-dimensional representation of Voronoi and Delaunay tessellations. The dashed lines show the Delaunay triangles and the solid lines show the Voronoi polygons. Π_i is given by OABCDE. The circum-circle centered at O for $t(i, j, k)$ is also shown. Points i, j, k are contiguous and their Voronoi polygons meet at the point O.

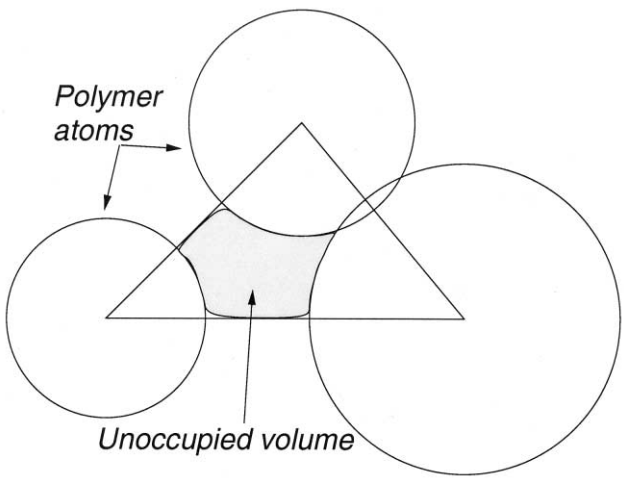

Fig. 2. Two-dimensional representation of unoccupied volume.

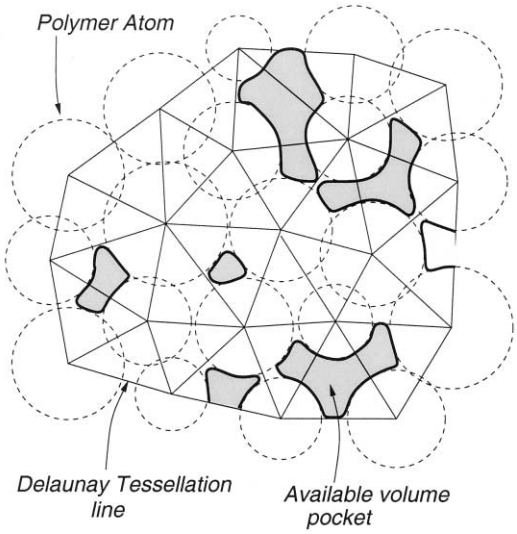

Fig. 3. Two-dimensional representation of available volume pockets.

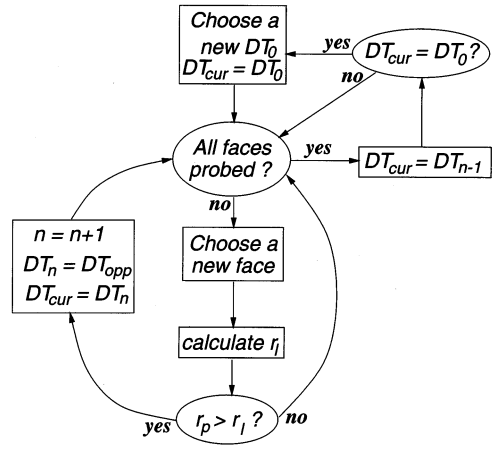

Fig. 5. Recursive algorithm used to evaluate each pocket of available volume.

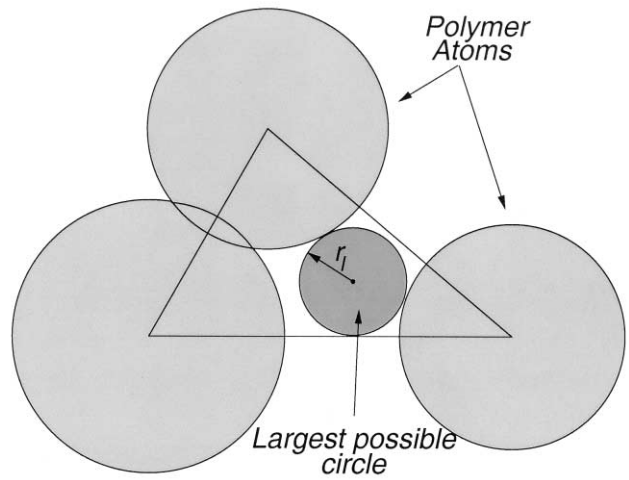

Fig. 4. Side of a DT. The darker circle represents the largest possible circle that can fit within the area of the face not occupied by the polymer atoms.

1. The model does not incorporate thermal motion. Temperature enters only indirectly through the specification of density.
2. The molecular structure is assumed to be in mechanical equilibrium, not thermal equilibrium (the glassy state by definition is a thermal non-equilibrium).
3. During the equilibration procedure, bond lengths and bond angles are considered to be fixed. Only the torsional angles are allowed to vary.
4. The polymer is assumed to be a periodic arrangement of several *amorphous cells*.

The software package INSIGHT from MSI Inc. has been used in this work. The procedure now involves the following four steps:

1. Generating the monomer structure from the chemical formula;

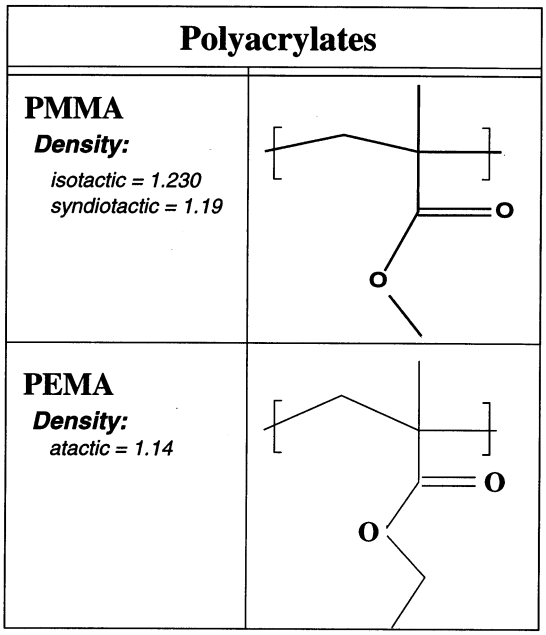

Fig. 6. Monomer structures of polycarbonates; brackets indicate the head and tail atoms.

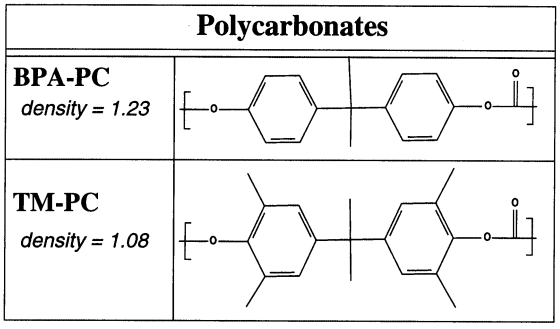

Fig. 7. Monomer structures of polyacrylates; brackets indicate the head and tail atoms.

2. Generating the polymer molecule from the monomer molecule;
3. Generating an initial guess structure of the amorphous cell by carefully assembling several polymer molecules; and
4. Equilibrating the amorphous structure to obtain the final structure.

The first two steps are fairly easy and can be implemented using the builder and polymerizer module in INSIGHT [5]. However, care is required in the second step to account for the tacticity of the polymer molecule. Since the bond angles and the bond lengths are not changed in the subsequent two steps, they need to be optimized at this stage. This is done using an appropriate force field.

Step 3 is the most crucial part of the procedure. It assures that the initial structure is not a very high energy structure. A high energy, initial structure most often produces, after minimization, a local minimum which is usually far from a realistic structure [3,6].

3. Structure analysis

Structures generated using the above procedure essentially yield the coordinates of the polymeric atomic sites. To draw any useful information from these structures, it is necessary to quantify their characteristics, which in turn needs a discretization procedure. To this end, we have chosen *Delaunay Tessellation* [7,8], as is defined below.

3.1. Delaunay tessellation

Let N points be distributed in a box V of finite size. Without loss of generality, let the box be a cube of side L ($|V| = L^3$). Let in V, x_1, x_2,... x_N be the position vectors of N points [8].

Consider a tetrahedron T whose vertices are the four points, i, j, k, and l. If the circumsphere of T is empty (i.e. it does not include any other points), then T is a Delaunay tetrahedron, often referred to as DT. The collection of all such tetrahedra forms a gapless tessellation called the Delaunay tessellation. i, j, k, l are said to be *contiguous* to each other.

The Delaunay tessellation is also *dual* to another tessellation called the *Voronoi tessellation*. Dual here means that, if one of these tessellations is known, then the other can be derived from it. Just as the Delaunay tessellation, the Voronoi tessellation is a gapless collection of the *Voronoi regions* (Π_i) each of which is defined as

$$\Pi_i = \{x | d(x, x_i) < d(x, x_j), \text{ for all } j \neq i\} \quad (1)$$

A 2-D representation of both tessellations is shown in Fig. 1. In the present case, the atomic centers are

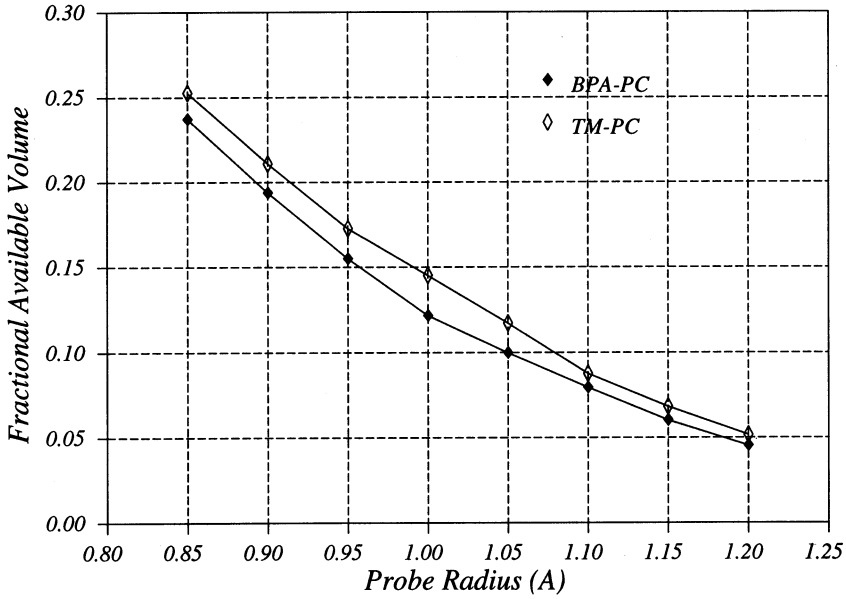

Fig. 8. Fractional available volume plots for TM-PC and BPA-PC.

considered to be the points distributed in the space. Each polymer atom is considered to be a rigid sphere of radius equal to 0.35 Å less than its Van der Waal radius. A new efficient three-dimensional algorithm is developed to calculate the Delaunay tessellation [9].

3.2. Available volume

As was mentioned earlier, an exact definition of free volume is not possible. Arizzi et al. [7] defined the unoccupied volume as the space available in each DT that is not occupied by the atoms (Fig. 2). They also analyzed the connectivity of these elements. Greenfield and Theodorou [10] probed the polymer structure with spheres of two different radii. They used a Monte Carlo-based clustering algorithm [11] to find the clusters of tetrahedra that are accessible to a probe.

Since the DTs are artificial entities, they should not influence the definition of the available volume. We define the available volume by means of probing the microstructure using spheres of different sizes. The structure is considered to contain discrete pockets of available volume, a 2-D representation of which is shown in Fig. 3. The available volume pockets shown in the figure are the regions through which the probing sphere can pass freely. Each of these pockets is determined using a recursive algorithm described below, for a probe of radius r_p. This algorithm automatically clusters together tetrahedra that are freely accessible to a probe of a given size into pockets without using a statistical approach. Though not necessary, one may interpret the pockets resulting from smaller probe radii as pathways (similar to the interpretation suggested by Greenfield and Theodorou [2]). Fig. 5 illustrates the algorithm. The following steps are required:

1. Choose an arbitrary DT_0 and add it to the current pocket. Let DT_{cur} be the DT whose faces are being currently probed.
2. Make $DT_{cur} = DT_0$.
3. Check if all faces have already been probed.
4. If not, choose a face and determine the largest possible circle (radius r_1) that can be fit within the area of the face not occupied by the polymer atoms (Fig. 4).

Table 1
Approximate diffusion coefficients of O_2 and CO_2

Polymer	O_2 ($D \times 10^8$ cm^2 s^{-1})	CO_2 ($D \times 10^8$ cm^2 s^{-1})
BPA-PC	5.6[a]	3.1[a]
TM-PC	8.11[a]	5.7[a]
iso-PMMA	0.23[b]	0.04[b]
syn-PMMA	0.40[b]	0.08[b]
PEMA	11.5[c]	3.0[c]

[a] From Ref. [12].
[b] From Ref. [13].
[c] From Ref. [14].

Table 2
Number of rotatable bonds per unit volume

Polymer	TNR[a] ($\times 10^3$)	NRM[b] ($\times 10^3$)
BPA-PC	22.709	5.677
TM-PC	23.905	12.950
iso-PMMA	44.302	14.676
syn-PMMA	43.300	14.334
PEMA	42.026	18.011

[a] TNR, total number of rotatable bonds per unit volume (A^3).
[b] NRM, number of rotatable bonds associated with methyl groups per unit volume (A^3).

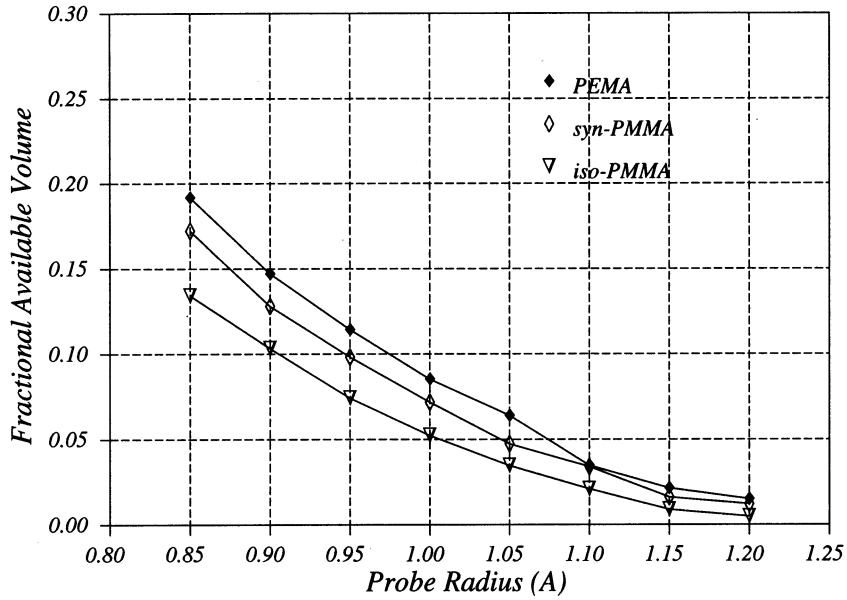

Fig. 9. Fractional available volume plots for iso-PMMA, syn-PMMA and PEMA.

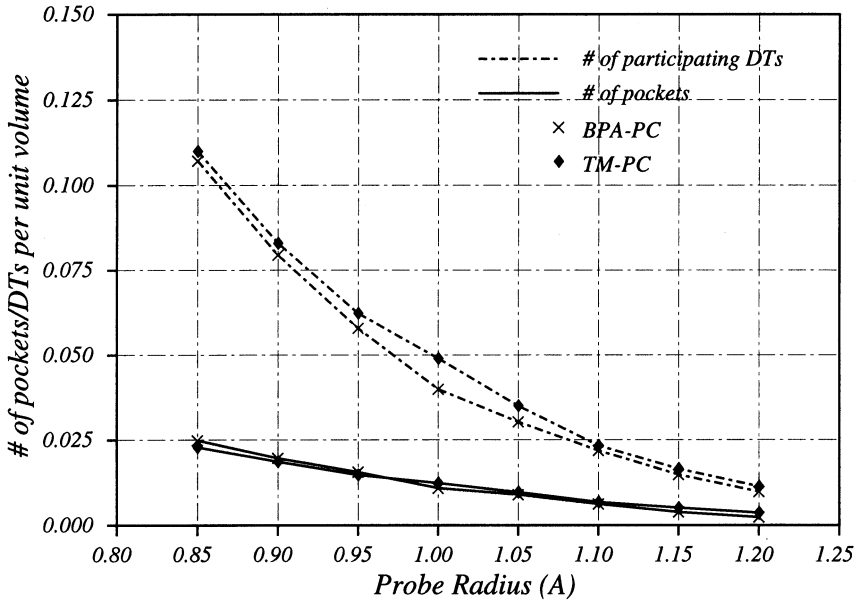

Fig. 10. Number of available volume pockets and DTs contributing to these pockets per unit volume for the polycarbonates.

4.1. If $r_l > r_p$ the probe is assumed to pass through the face. Add the adjacent DT which shares this face, referred to as DT_{opp}, to the pocket. Make $DT_{cur} = DT_{opp}$. Return to step 3.

4.2. If $r_l < r_p$, the probe is assumed not to pass through the face. Return to step 3.

5. If all faces have been probed, then proceed as follows:

5.1. Make DT_{cur} equal to the previous DT (DT_{n-1}) in the pocket.

5.2. Check if $DT_{cur} = DT_0$, i.e. if all the previous DTs in the pocket have been probed.

5.3. If yes, we are done with determining the current pocket. Store the pocket and start determining a new pocket, i.e. return to step 1.

5.4. If no, return to step 3.

One can immediately notice that the size of each of these pockets depends on the size of the probing sphere, which in general may be thought of as the diffusing molecule. Further, for a given structure, the available volume distribution is unique regardless of which starting DT the algorithm has chosen. Also, the tessellation merely assists one in evaluating the above distribution, and its contribution to the final results is minimal.

There may be several pockets which involve only one DT. For these we merely check if a sphere larger than or equal to the probe can fit into the unoccupied volume (Fig. 2) in the DT.

4. Polymer types

Four different polymers belonging to two different categories have been chosen. From polycarbonates, bisphenol polycarbonate (BPA-PC) and tetra-methyl polycarbonate (TM-PC) have been chosen. From polyacrylates, poly methyl methacrylate (PMMA) and poly ethyl methacrylate (PEMA) have been chosen. Figs. 6 and 7 show their monomer chemical structures. In the case of the acrylates, analysis has also been done for different tacticities.

5. Results and discussion

Fig. 8 shows the fractional available volume for BPA-PC and TM-PC plotted against the probe radius. It is seen that the difference in the fractional available volume between the two polymers is only marginal (1–2%) for all probe radii. This difference is smaller than that for the average free volumes estimated using the group contribution method [15]. However, as Table 1 shows, the average diffusion coefficient of TM-PC is approximately 1.5 times that of BPA-PC for most small molecules. It is possible that a significant contribution also comes from the flexibility of the additional methyl groups, which also tend to have a hole near them due to the relative inflexibility of the backbone. Table 2 gives a comparison between the number of rotatable bonds per unit volume between BPA-PC and TM-PC. The third column of the table shows the contribution to the number of rotatable bonds from the methyl groups. The methyl groups (Fig. 7) can be rotated very easily around their C–C bond between them and the backbone, with very little local configurational changes.

Fig. 9 shows the fractional available volume for iso-PMMA, syn-PMMA, and PEMA, plotted against the probe radius. As expected, syn-PMMA has a larger available volume than iso-PMMA, because of the hindrance between oppositely extending side chains during the polymer molecule packing. This difference is also reflected in their diffusion coefficient seen in Table 1. The difference in the available volume between the PEMA and syn-PMMA is slightly higher than that for BPA-PC and TM-PC. It is, however, not clear why the diffusion coefficients of PEMA and PMMA differ by almost an order of magnitude. This may be due to a specific way the polymer chains are packed in PMMA, which decreases the chain mobility significantly. However, small amounts of available volume in both PMMA and PEMA (relative to PCs) are supported by a small amount of solubility of most inert gases in the acrylates [14]. Further, both PEMA and PMMA seem to have similar solubility coefficients [13,14]. Comparable diffusion coefficients between the PCs and PEMA may be attributed to the larger flexibility of PEMA chains (Table 2).

Figs. 10 and 11 show the numbers of available volume pockets per unit volume and the number of DTs per unit volume contributing to these pockets. The amount of vertical gap between the upper curve (number of DTs contributing to the available volume pock-

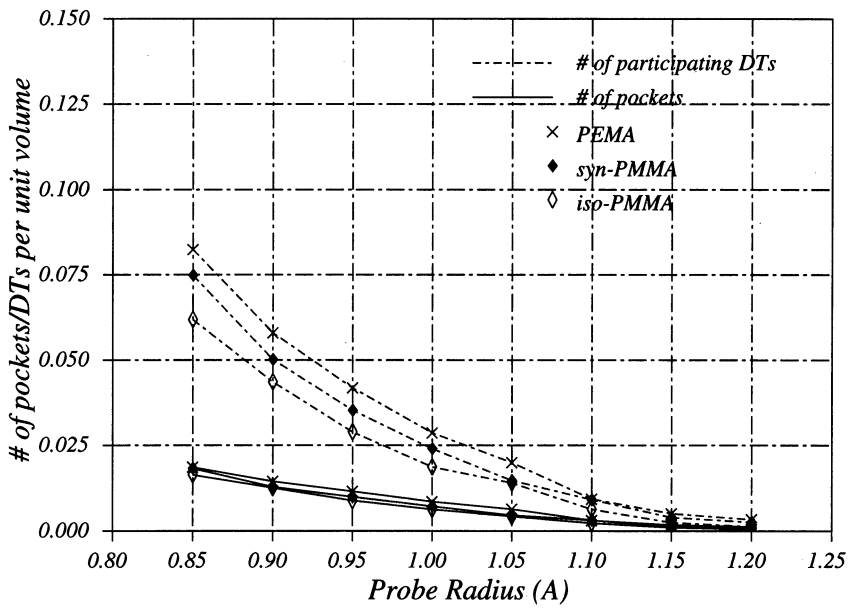

Fig. 11. Number of available volume pockets and DTs contributing to these pockets per unit volume for the acrylates.

ets) and the corresponding lower curve (number of available volume pockets), is an indirect measure of the average size of the available volume pockets. From Figs. 10 and 11, it is clear that the carbonates have larger numbers of pockets than the acrylates. Further, the average number of DTs per pocket is smaller for acrylates compared to the carbonates. This is expected since the acrylates, in general, are more flexible than the carbonates, allowing them to pack more closely than the carbonates, leaving smaller gaps.

Acknowledgements

This work has been supported by the Army Research Office (ARO) Contract DAAH04-95-1-0369 to the University of California, San Diego.

References

[1] A.A. Gusev, F. Muller-Plathe, W.F. van Gunsteren, U.W. Suter, Adv. Polym. Sci. 116 (1994) 207–247.
[2] M.L. Greenfield, D.N. Theodorou, Macromolecules 31 (1998) 7068–7090.
[3] D.N. Theodorou, U.W. Suter, Macromolecules 18 (1985) 1467–1478.
[4] W.L. Mattice, U.W. Suter, Conformational Theory of Large Molecules: The Rotational Isomeric State Model in Macromolecular Systems, Wiley, New York, 1994.
[5] Manual-B. InsightII: Polymerizer Module. Molecular Simulations Inc. (MSI), 9685 Scranton Road, San Diego, CA 92121, 1998.
[6] Manual-A. InsightII: Amorphous Cell Module. Molecular Simulations Inc. (MSI), 9685 Scranton Road, San Diego, CA 92121, 1998.
[7] S. Arizzi, P.H. Mott, U.W. Suter, J. Polym. Phys. B Polym. Phys. 30 (1992) 415–426.
[8] M. Tanemura, T. Ogawa, N. Ogita, J. Comput. Phys. 51 (1983) 191–207.
[9] S. Putta, S. Nemat-Nasser. A new 3-D algorithm to determine Voronoi and Delaunay tessellation, in preparation, 1999.
[10] M.L. Greenfield, D.N. Theodorou, Macromolecules 26 (1993) 5461–5472.
[11] E.M. Sevick, P.A. Monson, J.M. Ottino, J. Chem. Phys. 88 (1988) 1198–1206.
[12] W.J. Koros, G.L. Fleming, S.M. Jordon, T.H. Kim, H.H. Hoehn, Prog. Polym. Sci. 13 (1988) 339–401.
[13] K.E. Min, D.R. Paul, J. Polym. Sci. B Polym. Phys. 26 (1988) 1021–1033.
[14] J.S. Chiou, D.R. Paul, J. Membr. Sci. 45 (1989) 167–189.
[15] M. Aguilar-Vega, D.R. Paul, J. Polym. Sci. B Polym. Phys. 31 (1993) 1599–1610.